



Effects of Cu additions on mechanical and soft-magnetic properties of CoFeBSiNb bulk metallic glasses

Genlei Zhang^{a, b}, Qianqian Wang^{a, b}, Chenchen Yuan^{a, b}, Weiming Yang^c, Jing Zhou^{a, b}, Lin Xue^{a, b}, Feng Hu^{a, b}, Baoan Sun^d, Baolong Shen^{a, b, c, *}

^a School of Materials Science and Engineering, Southeast University, Nanjing 211189, China

^b Jiangsu Key Laboratory for Advanced Metallic Materials, Nanjing 211189, China

^c Institute of Massive Amorphous Metal Science, China University of Mining and Technology, Xuzhou 221116, China

^d Herbert Gleiter Institute of Nanoscience, Nanjing University of Science and Technology, Nanjing 210094, China

ARTICLE INFO

Article history:

Received 29 September 2017

Received in revised form

14 December 2017

Accepted 16 December 2017

Available online 18 December 2017

Keywords:

Co-based bulk metallic glasses

Plasticity

Nano-scale precipitation phase

Shear bands

ABSTRACT

A novel ductile $[(\text{Co}_{0.7}\text{Fe}_{0.3})_{0.68}\text{B}_{0.219}\text{Si}_{0.051}\text{Nb}_{0.05}]_{99.5}\text{Cu}_{0.5}$ bulk metallic glass (BMG) with the strength of 4.4 GPa and the compressive plastic strain of 2.5% was successfully synthesized in this work. We found, by adding tiny Cu (0–0.9 at. %) element, both the plasticity and the saturation magnetization of CoFeBSiNb BMGs can be improved, which is attributed to the existence of ferromagnetic and ductile α -(Fe, Co) nanoparticles in the glass matrix. The abundant of vein patterns and high-density multiple shear bands were observed on the fracture surface of Cu-added Co-based bulk glassy rods. The reason for these results is that the nanoscale particles hinder the propagation of the shear band, promote the generation of multiple shear bands and enhance the plasticity. Our investigations shade a light on understanding the nano-scale precipitation phase enhanced ductility mechanism in high strength BMGs such as Fe- and Co-based BMGs and lead a map for finding new high strength BMGs with high plasticity.

© 2017 Elsevier B.V. All rights reserved.

1. Introduction

Since the first exploration of the Co-based bulk metallic glasses (BMGs) in 2001 [1], a series of Co-based BMGs systems have been synthesized [2–5]. Compared to other BMGs, Co-based BMGs have excellent magnetic properties, i.e., high saturation magnetization (B_s), high effective permeability (μ_e) and low coercivity (H_c) [6–8]. On the other hand, these alloy systems also exhibit superior mechanical properties, i.e., high fracture strength (σ_f) and high hardness [9–11]. Due to the excellent magnetic and mechanical properties, Co-based BMGs have attracted attentions for engineering applications as structural and functional materials. However, the macroscopic plastic deformation ability of the Co-based BMGs is very limited or the alloy systems even do not present ductile behavior at room temperature, which results in catastrophic fracture in these alloys [12], and prevents their wide applications as new structural materials. Therefore, it is urgent to improve the plasticity of Co-based BMGs at room temperature while

maintaining superior soft magnetic properties.

Recently, compressive plastic deformation ability has been improved in Zr- [13,14], Cu- [15–17], Ni- [18,19], Ti- [20,21], Mg- [22] and Pd-based [23] BMGs composites by producing second dendrites, particle phases, or fine pore phases in the glass matrices. In addition, for ferromagnetic BMGs, it was found that the addition of a certain amount of alloying element such as Cu could improve the plasticity of Fe-based BMGs by introducing crystalline phases. Shen et al. [24] reported distinct enhancement of compressive plasticity by adding 0.25 at. % Cu in the FeCoBSiNb BMGs. The structure studies showed that microcrystalline grains α -(Fe, Co) and $(\text{Fe, Co})_{23}\text{B}_6$ *in situ* precipitated in the BMGs matrix. Li et al. [25] studied the effect of adding a small amount of Cu (0.1–0.6 at. %) on the plastic properties of FeSiBP bulk metallic glasses; they found that the plastic strain of this alloy system was enhanced by the addition of Cu. It was observed that a large number of α -(Fe, Co) nanocrystalline grains dispersed in the glassy matrix, which promote the generation of multiple shear bands and prevent the sudden brittle fracture of the FeSiBP samples. The large plastic deformation was attributed to the generation and movement of the multiple shear bands because of the existence of crystalline phase. However, rare report has been found about the secondary phase

* Corresponding author. School of Materials Science and Engineering, Southeast University, Nanjing 211189, China.

E-mail address: blshen@seu.edu.cn (B. Shen).

enhancing plasticity in Co-based BMGs. It has been reported that the mixing enthalpy of Fe–Cu (+13 kJ/mol), Co–Cu (+6 kJ/mol) and Nb–Cu (+3 kJ/mol) atomic pairs [26] are positive. Thereby, Cu is hardly soluble in Fe at room temperature [27], which has been proven to be beneficial to precipitate the second phases.

In this work, for improving the plasticity of Co-based BMGs by the second phases dispersed in their substrate, a small amount of Cu was added to the $(\text{Co}_{0.7}\text{Fe}_{0.3})_{0.68}\text{B}_{0.219}\text{Si}_{0.051}\text{Nb}_{0.05}]_{100-x}\text{Cu}_x$ BMG [12] with high GFA. The present Co-based BMGs simultaneously possess super-high strength and enhanced plasticity, offering great benefits in engineering the strength of Co-based BMGs and opening new avenues for improving their plasticity.

2. Experimental

Multi-component alloy ingots with nominal compositions $[(\text{Co}_{0.7}\text{Fe}_{0.3})_{0.68}\text{B}_{0.219}\text{Si}_{0.051}\text{Nb}_{0.05}]_{100-x}\text{Cu}_x$ ($x = 0, 0.1, 0.3, 0.5, 0.7, 0.9$) were prepared by arc melting mixtures of pure Co (99.99 wt%), Fe (99.99 wt%), B (99.999 wt%), Si (99.99 wt%), Nb (99.95 wt%), Cu (99.995 wt%) in a high purity argon atmosphere. Ribbons with thickness of 33 μm and width of 1.3 mm were produced by single roller melt-spinning method. The cylindrical rods with diameters up to 3.5 mm were fabricated by a copper mold casting method. The structure of as-quenched specimens was identified by X-ray diffraction (XRD) with Cu-K α radiation. The thermal stability associated with glass transition temperature (T_g), crystallization temperature (T_x), melting temperature (T_m) of the amorphous samples was examined by NETZSCH 404 F3 differential scanning calorimeter (DSC) at a heating rate of 0.67 K/s, while liquidus temperature (T_l) was tested by DSC at a cooling rate of 0.067 K/s. The fracture strength (σ_f) and compressive plastic strain (ϵ_p) were measured at room temperature by compressive testing with an Instron testing machine. The gauge size of bulk glassy rods for compressive testing was 1 mm in diameter and 2 mm in length. The compressive strain rate was $5 \times 10^{-4} \text{ s}^{-1}$. The deformation and fracture surface morphology were observed by scanning electron microscopy (SEM). The microstructures of bulk glassy rods were examined with high resolution transmission electron microscope (TEM). For TEM measurements, the rod specimens were first prepared carefully by the mechanical thinning of the discs to a thickness of 40 μm , and then by the low-angle (5°) ion milling thinning for about 180 min using a Gatan 691 Precision Ion Polishing System. The ribbon samples for magnetic property measurements were annealed for 300 s at the temperature of $T_g - 50 \text{ K}$ for improving soft-magnetic properties through structural relaxation. Then the saturation magnetization (B_s) was measured using a vibrating sample magnetometer (VSM) under the maximum applied field of 800 kA/m. The coercivity (H_c) of amorphous ribbons with the length of 70 mm was measured using a DC B-H loop tracer under a maximum field of 800 A/m.

3. Results and discussion

The as-cast $[(\text{Co}_{0.7}\text{Fe}_{0.3})_{0.68}\text{B}_{0.219}\text{Si}_{0.051}\text{Nb}_{0.05}]_{100-x}\text{Cu}_x$ ($x = 0, 0.1, 0.3, 0.5, 0.7, 0.9$) alloys have relatively large glass forming ability (GFA), which leads to large critical diameters of rod specimens (5.5, 5.5, 4.5, 4.5, 4.5 and 3.5 mm, respectively), characterized as metallic glasses by XRD analysis, as shown in Fig. 1. The XRD patterns reveal only one typical halo without appearance of peaks corresponding to crystalline phases, indicating that these cylindrical alloy rods essentially consist of a single amorphous structure.

Fig. 2 shows DSC curves of the melt-spun $[(\text{Co}_{0.7}\text{Fe}_{0.3})_{0.68}\text{B}_{0.219}\text{Si}_{0.051}\text{Nb}_{0.05}]_{100-x}\text{Cu}_x$ ($x = 0, 0.1, 0.3, 0.5, 0.7, 0.9$) glassy alloy ribbons. All the alloys exhibit distinct glass transition, followed by a supercooled liquid region, and then crystallization which

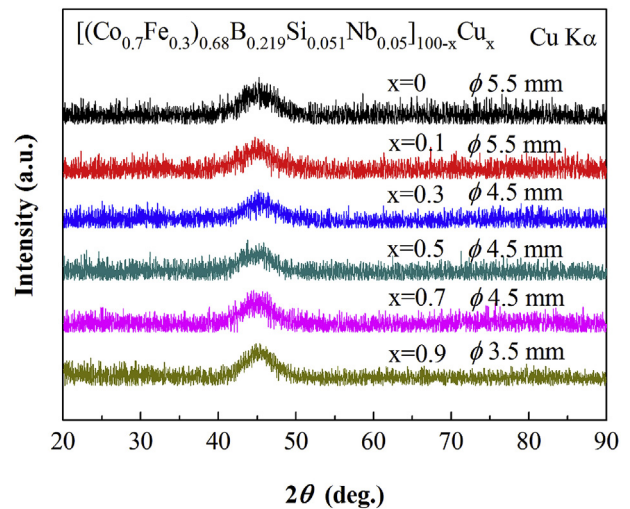


Fig. 1. XRD patterns of the as-cast $[(\text{Co}_{0.7}\text{Fe}_{0.3})_{0.68}\text{B}_{0.219}\text{Si}_{0.051}\text{Nb}_{0.05}]_{100-x}\text{Cu}_x$ ($x = 0, 0.1, 0.3, 0.5, 0.7, 0.9$) rods with critical diameters.

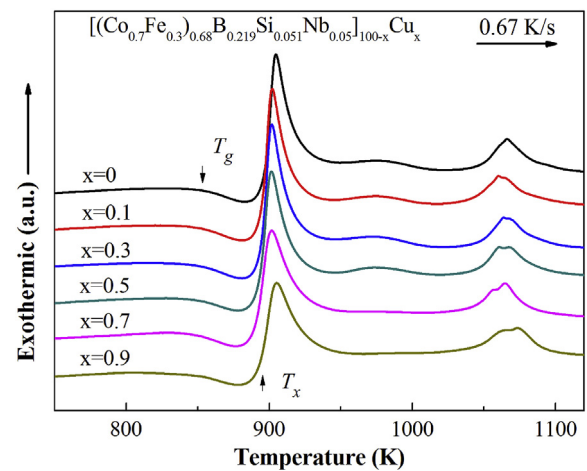


Fig. 2. DSC traces for the as-cast $[(\text{Co}_{0.7}\text{Fe}_{0.3})_{0.68}\text{B}_{0.219}\text{Si}_{0.051}\text{Nb}_{0.05}]_{100-x}\text{Cu}_x$ ($x = 0, 0.1, 0.3, 0.5, 0.7, 0.9$) glassy alloys at heating rate of 0.67 K/s.

corresponding to the precipitation of α -(Fe, Co) and $(\text{Fe, Co})_{23}\text{B}_6$ phases in this type of alloy [24,28,29]. The thermal parameters of the Co-based BMGs are summarized in Table 1. For all the alloy compositions, with the increase of Cu content from 0 to 0.9 at. %, T_g gradually decreases from 854 to 847 K, while T_x also reduces from 896 to 889 K, with a supercooled liquid region of 42 K, approximately. The liquidus temperature (T_l) values lie between 1313 and 1353 K. With the increase of Cu content from 0 to 0.7 at. %, T_l decreases from 1353 to 1313 K, which indicates that the alloy is gradually close to the eutectic point. The reduced glass transition temperatures (T_g/T_l) of these metallic glasses lie in a high value range of 0.63–0.65.

The stress-strain curves of the Co-based bulk metallic glasses were obtained by uniaxial compression tests performed at room temperature, as shown in Fig. 3. The fracture strength and the plastic strain of the $[(\text{Co}_{0.7}\text{Fe}_{0.3})_{0.68}\text{B}_{0.219}\text{Si}_{0.051}\text{Nb}_{0.05}]_{100-x}\text{Cu}_x$ ($x = 0, 0.1, 0.3, 0.5, 0.7, 0.9$) glassy rods are also listed in Table 1. The alloys exhibit high fracture strength of 4310–4400 MPa. The plastic strain for BMGs without Cu was 0.8% and increases to 1.0%, 1.4%, 2.5%, 1.2% and 0.9% for the 0.1 at. %, 0.3 at. %, 0.5 at. %, 0.7 at. % and 0.9 at. % Cu-added BMGs, respectively. The

Table 1

Critical diameters, thermal stability, mechanical properties, and magnetic properties of the as-cast $[(\text{Co}_{0.7}\text{Fe}_{0.3})_{0.68}\text{B}_{0.219}\text{Si}_{0.051}\text{Nb}_{0.05}]_{100-x}\text{Cu}_x$ ($x = 0, 0.1, 0.3, 0.5, 0.7, 0.9$) metallic glasses.

Cu content	T_g (K)	T_x (K)	ΔT (K)	T_m (K)	T_i (K)	T_g/T_i	H_c (A/m)	B_s (T)	σ_f (MPa)	ϵ_p (%)	D_{cr} (mm)
$x = 0$	854	896	42	1294	1320	0.65	0.78	0.70	4320	0.8	5.5
$x = 0.1$	853	894	41	1294	1353	0.63	0.81	0.73	4330	1.0	5.5
$x = 0.3$	853	893	40	1292	1331	0.64	1.27	0.73	4370	1.4	4.5
$x = 0.5$	850	892	42	1290	1316	0.65	1.32	0.73	4400	2.5	4.5
$x = 0.7$	848	889	41	1289	1313	0.65	1.41	0.72	4310	1.2	4.5
$x = 0.9$	847	889	42	1289	1315	0.64	1.85	0.69	4330	0.9	3.5

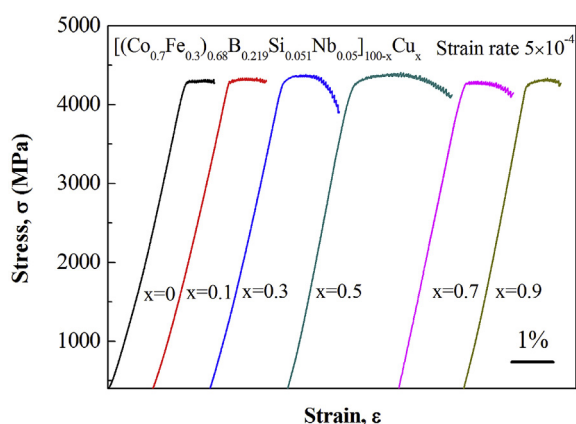


Fig. 3. Compressive stress-strain curves of $[(\text{Co}_{0.7}\text{Fe}_{0.3})_{0.68}\text{B}_{0.219}\text{Si}_{0.051}\text{Nb}_{0.05}]_{100-x}\text{Cu}_x$ ($x = 0, 0.1, 0.3, 0.5, 0.7, 0.9$) glassy rods with the diameter of 1 mm.

$[(\text{Co}_{0.7}\text{Fe}_{0.3})_{0.68}\text{B}_{0.219}\text{Si}_{0.051}\text{Nb}_{0.05}]_{99.5}\text{Cu}_{0.5}$ alloy exhibits larger plasticity than the others. The results demonstrate that properly adding a small amount of Cu element can significantly improve the plasticity of Co-based BMGs.

Fig. 4 shows SEM images of the $[(\text{Co}_{0.7}\text{Fe}_{0.3})_{0.68}\text{B}_{0.219}\text{Si}_{0.051}\text{Nb}_{0.05}]_{99.5}\text{Cu}_{0.5}$ surface prior to failure subjected to compression test. The outer surface and fracture surface of this Co-based bulk glassy alloy are shown in Fig. 4 (a) and (c), respectively, together with their partially enlarged details (Fig. 4 (b) and (d), respectively). There are high-density shear bands distributing on the sample surface, including the main shear band and massive secondary shear bands. The secondary shear bands intersect with the main shear band, as well as themselves (Fig. 4 (b)). These intricate shear bands make alloys avoid catastrophic fracture and exhibit certain degree of plastic deformation. The fracture surfaces exhibit well-developed vein patterns (Fig. 4 (d)), which are common characteristics observed on ductile non-ferrous BMGs. In addition, there are small droplets formed by melting on the compression fracture surface, which indicates that the shearing deformation of alloy accompanies adiabatic heating during compression. In general, the number of shear bands determines the plastic deformation ability of the BMGs. During the compressive process, the plastic deformation is largely confined into the shear bands, and then the shear bands will rapidly expand until sudden fracture. These results further convince that the promotion of multiple shear bands is an effective method to increase the plasticity of the Co-based bulk glassy alloys. And the plasticity is attributed to the abundant vein patterns, as well as the generation and propagation of high-density multiple shear bands, which are closely related to the precipitates in the alloys. Therefore, large plastic deformation can be obtained by adding appropriate Cu in the Co-based alloys.

To further explain the origin of the fracture of the Cu-added Co-based BMGs, the microstructure of the rod specimens with critical

diameters (5.5, 4.5 and 3.5 mm for alloys with $x = 0, 0.5$ and 0.9 , respectively) was carefully examined with high resolution TEM. Fig. 5 shows the TEM images and the selected area electron diffraction (SAED) of the BMGs $[(\text{Co}_{0.7}\text{Fe}_{0.3})_{0.68}\text{B}_{0.219}\text{Si}_{0.051}\text{Nb}_{0.05}]_{100-x}\text{Cu}_x$ rod specimens: (a) $x = 0$; (b) $x = 0.5$ and (c) $x = 0.9$. In Fig. 5 (a), the TEM diffraction patterns show that the amorphous structure of the investigated samples. When a small amount of Cu ($x = 0.5$) is added into the Co-based BMGs, a large number of α -(Fe, Co) with diameters of less than 5 nm dispersing in the amorphous matrix are observed in the TEM image and its selected diffraction pattern, as shown in Fig. 5 (b1) and (b2), respectively. With a Cu content up to 0.9 at. %, some dendrites ($(\text{Fe, Co})_{15}\text{Si}_3\text{B}_2$ and $(\text{Fe, Co})_3\text{B}$) larger than 200 nm in size are observed besides the α -(Fe, Co), as shown in Fig. 5 (c1) and (c2), respectively.

From the above results and discussion, an explanation of the deformation mechanism can be drawn, as shown in Fig. 6. According to the schematic diagrams describing the change of internal composition and structure in the compressed samples, the mechanism for plastic deformation of Co-based BMGs is revealed. Taking $[(\text{Co}_{0.7}\text{Fe}_{0.3})_{0.68}\text{B}_{0.219}\text{Si}_{0.051}\text{Nb}_{0.05}]_{99.5}\text{Cu}_{0.5}$ for an example, since Cu is hardly soluble in Fe at room temperature, there are many inhomogeneous Cu clusters (the orange circles in Fig. 6) dispersing in the BMG substrate, as shown in Fig. 6 (a). At the beginning of the compression, the shear bands are activated at the central position of the sample. But initial stress only leads to a small number and simple form of shear bands. It has been reported that the temperature in the vicinity of high stress would increase rapidly during compression [30]. Thus, Cu clusters may act as nucleation sites of α -(Fe, Co) and nanocrystallization possibly takes place during compression. A small number of α -(Fe, Co) nuclei (red circle in Fig. 6) are produced around the Cu clusters, as shown in Fig. 6 (b). The shear bands gradually expand as the load continuously increases. During compression, a large number of shear bands are produced and interact with ductile nanoscale crystalline phases, resulting in the shear bands branching. The shear bands of these branches cross each other, hindering further deformation until fracture, as shown in Fig. 6 (c)–(e). Thus, the formation of abundant of branching shear bands results in the improvement of the plasticity. However, when the Cu content exceeds a certain amount, complicated multiple crystalline phases or some dendrites may be produced during compression, which will deteriorate the properties of the alloy and cause the decrease of plasticity.

Fig. 7 shows the hysteresis loops of the $[(\text{Co}_{0.7}\text{Fe}_{0.3})_{0.68}\text{B}_{0.219}\text{Si}_{0.051}\text{Nb}_{0.05}]_{100-x}\text{Cu}_x$ ($x = 0, 0.1, 0.3, 0.5, 0.7, 0.9$) metallic glasses. It can be seen the magnetization quickly saturates under the applied magnetic field, which indicates excellent soft magnetic properties of the Co-based BMGs system. The B_s lies in a high value range from 0.70 to 0.74 T. Moreover, the H_c of the alloys are small, this may own to the structural relaxation after annealing [31]. The H_c increases gradually with the increase of Cu content as shown by the red line in Fig. 8. It may attribute to the addition of Cu which results in the nucleation sites formation of some α -(Fe, Co) and/or $(\text{Fe, Co})_3\text{B}$. The number of α -(Fe, Co) generally increases with the addition of Cu.

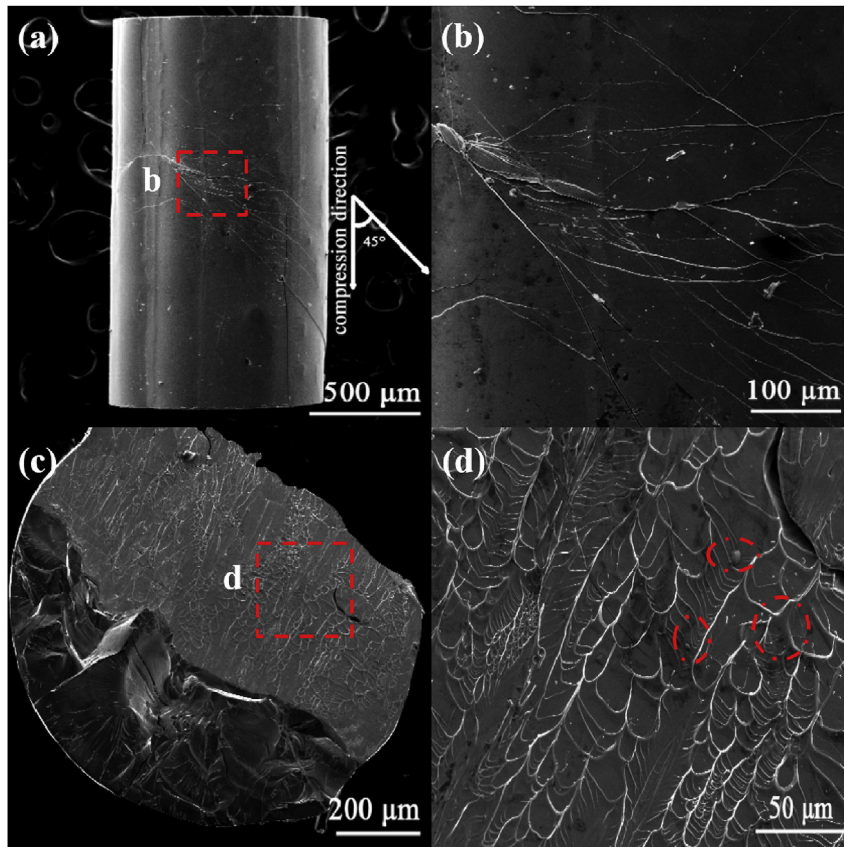


Fig. 4. SEM images of (a) multiple shear bands on the outer surface and (b) vein pattern on the fracture surface of the $[(\text{Co}_{0.7}\text{Fe}_{0.3})_{0.68}\text{B}_{0.219}\text{Si}_{0.051}\text{Nb}_{0.05}]_{99.5}\text{Cu}_{0.5}$ rod specimen; (b) and (d) are the enlarged b and d in the (a) and (c), respectively.

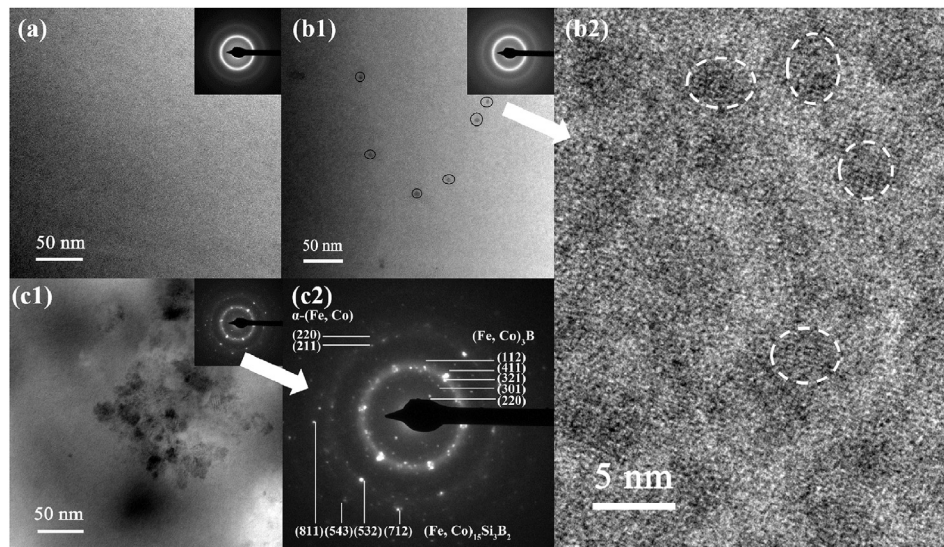


Fig. 5. TEM images and SAED patterns of the $[(\text{Co}_{0.7}\text{Fe}_{0.3})_{0.68}\text{B}_{0.219}\text{Si}_{0.051}\text{Nb}_{0.05}]_{100-x}\text{Cu}_x$ glassy rods with composition of (a) $x = 0$; (b) $x = 0.5$; (c) $x = 0.9$.

When the Cu content exceeds a certain value, chemical clusters of (Fe, Co) B may appear [32,33], which makes the H_c of the alloy increase further. Therefore, the precipitation of $\alpha\text{-(Fe, Co)}$, chemical clusters of (Fe, Co) B in the glassy matrix obviously increases the value of H_c . However, the B_s shows a trend of firstly increasing and then decreasing, which is different from that of the H_c . With the

increase of Cu content, the appearance of $\alpha\text{-(Fe, Co)}$ may be conducive to the improvement of B_s of the as-cast alloys. After adding more than a certain amount of Cu, (Fe, Co) B and other crystalline phases are detrimental to B_s of alloys [34]. This is almost consistent with the trend of the plasticity with Cu content, as shown by the blue line in Fig. 8.

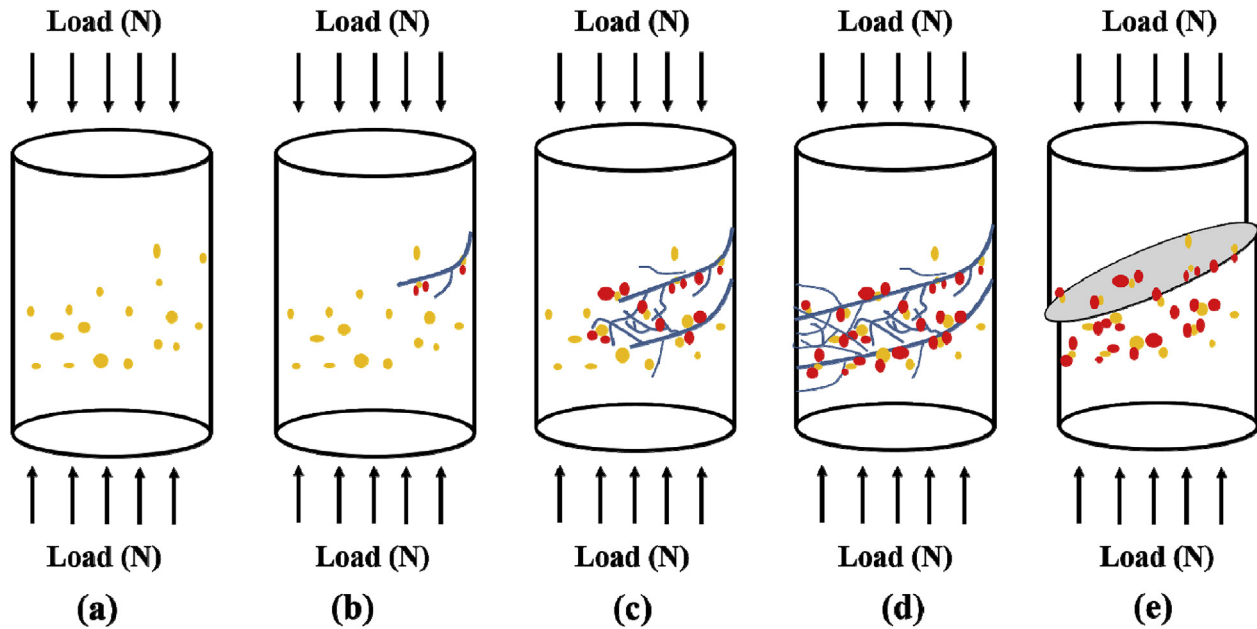


Fig. 6. Schematic diagrams of the internal composition and structure of $[(\text{Co}_{0.7}\text{Fe}_{0.3})_{0.68}\text{B}_{0.219}\text{Si}_{0.051}\text{Nb}_{0.05}]_{99.5}\text{Cu}_{0.5}$ glassy rods during compression. The orange circles and red circles represent Cu clusters and α -(Fe, Co), respectively. (For interpretation of the references to colour in this figure legend, the reader is referred to the Web version of this article.)

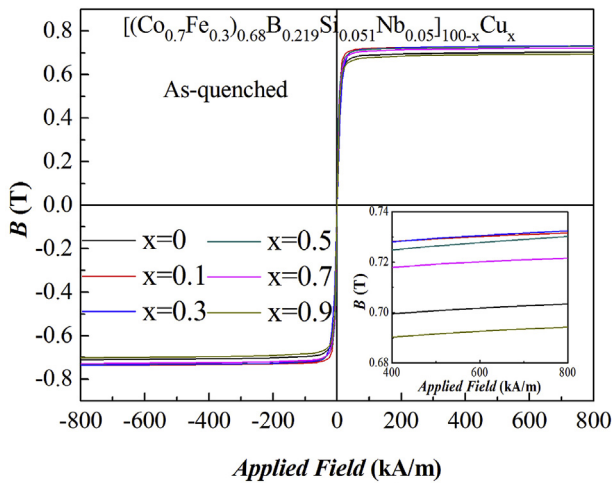


Fig. 7. Hysteresis loops of melt-spun $[(\text{Co}_{0.7}\text{Fe}_{0.3})_{0.68}\text{B}_{0.219}\text{Si}_{0.051}\text{Nb}_{0.05}]_{100-x}\text{Cu}_x$ ($x = 0, 0.1, 0.3, 0.5, 0.7, 0.9$) glassy ribbons measured by VSM.

The positive mixing enthalpy of the Fe-Cu, Co-Cu and Nb-Cu atomic pairs results in mutual repulsion in BMGs. Therefore, some Cu clusters may be embedded in the BMGs matrix, which act as nucleation sites of α -(Fe, Co) and other crystalline phases. In addition, the temperature near the region of high stress increases rapidly during the compression. This phenomenon is demonstrated by the small droplets observed in our experiment. So, crystallization at the nanoscale may occur during this process. During the compression, the shear bands interact with these nanoscale ductile crystal phases, bypassing/cutting through the ductile crystalline phase. This leads to the deflection of extension direction of the existed shear bands and then multiple shear bands are generated, which improve the plasticity of bulk glassy alloys. Therefore, a method of generating multiple shear bands by stress-induced nanocrystallization can improve the plasticity of the Co-based BMGs.

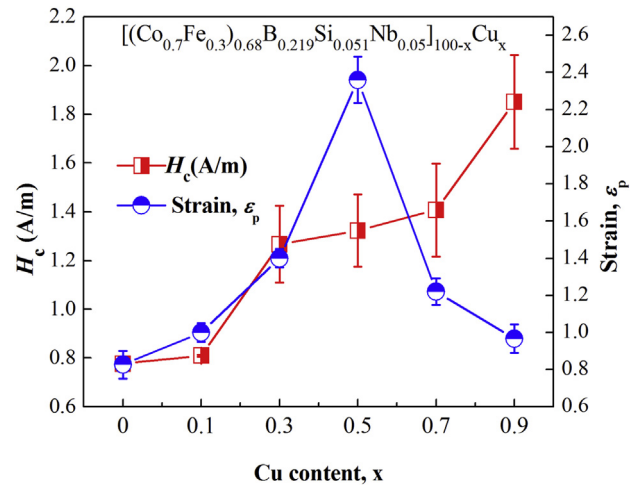


Fig. 8. The change of coercivity and plasticity with Cu content in $[(\text{Co}_{0.7}\text{Fe}_{0.3})_{0.68}\text{B}_{0.219}\text{Si}_{0.051}\text{Nb}_{0.05}]_{100-x}\text{Cu}_x$ ($x = 0, 0.1, 0.3, 0.5, 0.7, 0.9$) glassy alloys.

4. Conclusion

In this work, $[(\text{Co}_{0.7}\text{Fe}_{0.3})_{0.68}\text{B}_{0.219}\text{Si}_{0.051}\text{Nb}_{0.05}]_{100-x}\text{Cu}_x$ ($x = 0, 0.1, 0.3, 0.5, 0.7, 0.9$) alloys were prepared by copper mold casting with critical diameter up to 5.5 mm. With the Cu addition, the Co-based BMGs exhibit superior mechanical properties, such as superhigh σ_f of 4310–4400 MPa and large ϵ_p successfully elevated to 2.5%, and excellent magnetic properties, such as low H_c of 0.78–1.85 A/m, high B_s of 0.70–0.74 T. It is found that the mechanical and magnetic properties are closely correlated with their inner atomic cluster structure. The existence of α -(Fe, Co) is effective in improving not only B_s , but also the plasticity of the alloy by producing abundant of vein patterns on the fracture surface and a high density multiple shear bands on the flank of the rod specimen. The high strength together with the promising plasticity is encouraging for further development of Co-based BMGs with

potential applications.

Acknowledgement

This work was supported by the National Natural Science Foundation of China (Grant Nos. 51501037, 51601038 and 51631003), the Natural Science Foundation of Jiangsu Province, China (Grant No. BK20171354), the State Key Development Program for Basic Research of China (Grant No. 2016YFB0300502), the Fundamental Research Funds for the Central Universities (Grant No. 2242017K40189) and Jiangsu key laboratory for advanced metallic materials (Grant No. BM2007204).

References

- [1] B.L. Shen, H. Koshihara, A. Inoue, Bulk glassy $\text{Co}_{43}\text{Fe}_{20}\text{Ta}_{5.5}\text{B}_{31.5}$ alloy with high glass-forming ability and good soft magnetic properties, *Mater. Trans.* 42 (2001) 2136–2139.
- [2] A. Inoue, B.L. Shen, H. Koshihara, Cobalt-based bulk glassy alloy with ultrahigh strength and soft magnetic properties, *Nat. Mater.* 2 (2003) 661–663.
- [3] A. Inoue, B.L. Shen, H. Koshihara, Ultra-high strength above 5000 MPa and soft magnetic properties of Co-Fe-Ta-B bulk glassy alloys, *Acta Mater.* 52 (2004) 1631–1637.
- [4] C.T. Chang, B.L. Shen, A. Inoue, Co-Fe-B-Si-Nb bulk glassy alloys with super-high strength and extremely low magnetostriction, *Appl. Phys. Lett.* 88 (2006), 011901.
- [5] K. Amiya, A. Urata, N. Nishiyama, Magnetic properties of Co-Fe-B-Si-Nb bulk glassy alloy with zero magnetostriction, *J. Appl. Phys.* 101 (2007), 09N112.
- [6] Y.Q. Dong, Q.K. Man, H.J. Sun, B.L. Shen, S.J. Pang, T. Zhang, A. Makino, A. Inoue, Glass-forming ability and soft magnetic properties of $(\text{Co}_{0.6}\text{Fe}_{0.3}\text{Ni}_{0.1})_{67}\text{B}_{22+x}\text{Si}_{6-x}\text{Nb}_5$ bulk glassy alloys, *J. Alloys Compd.* 509 (2011) S206–S209.
- [7] A. Inoue, F.L. Kong, Q.K. Man, B.L. Shen, R.W. Li, F. Al-Marzouki, Development and applications of Fe- and Co-based bulk glassy alloys and their prospects, *J. Alloys Compd.* 615 (2014) S2–S8.
- [8] Y.Q. Dong, Q.K. Man, C.T. Chang, B.L. Shen, X.M. Wang, R.W. Li, Preparation and magnetic properties of $(\text{Co}_{0.6}\text{Fe}_{0.3}\text{Ni}_{0.1})_{70-x}(\text{B}_{0.811}\text{Si}_{0.189})_{25+x}\text{Nb}_5$ bulk glassy alloys, *J. Mater. Sci. Mater. Electron.* 26 (2015) 7006–7012.
- [9] J.F. Wang, R. Li, N.B. Hua, T. Zhang, Co-based ternary bulk metallic glasses with ultrahigh strength and plasticity, *J. Mater. Res.* 26 (2011) 2072–2079.
- [10] J.F. Wang, L. Huang, S.J. Zhu, Q.K. Li, S.K. Guan, T. Zhang, Glass-forming ability, fragility parameter, and mechanical properties of Co-Ir-Ta-B amorphous alloys, *J. Alloys Compd.* 576 (2013) 375–379.
- [11] C.C. Dun, H.S. Liu, L. Hou, L. Xue, L.T. Dou, W.M. Yang, Y.C. Zhao, B.L. Shen, Ductile Co-Nb-B bulk metallic glass with ultrahigh strength, *J. Non Cryst. Solids* 386 (2014) 121–123.
- [12] Y.Q. Dong, A.D. Wang, Q.K. Man, B.L. Shen, $(\text{Co}_{1-x}\text{Fe}_x)_{68}\text{B}_{21.9}\text{Si}_{5.1}\text{Nb}_5$ bulk glassy alloys with high glass-forming ability, excellent soft-magnetic properties and superhigh fracture strength, *Intermetallics* 23 (2012) 63–67.
- [13] C.C. Hays, C.P. Kim, W.L. Johnson, Microstructure controlled shear band pattern formation and enhanced plasticity of bulk metallic glasses containing *in situ* formed ductile phase dendrite dispersions, *Phys. Rev. Lett.* 84 (2000) 2901–2904.
- [14] C. Fan, R.T. Ott, T.C. Hufnagel, Metallic glass matrix composite with precipitated ductile reinforcement, *Appl. Phys. Lett.* 81 (2002) 1020–1022.
- [15] Y.C. Kim, D.H. Kim, J.C. Lee, Formation of ductile Cu-based bulk metallic glass matrix composite by Ta addition, *Mater. Trans.* 44 (2003) 2224–2227.
- [16] A. Inoue, W. Zhang, T. Tsurui, A.R. Yavari, A.L. Greer, Unusual room-temperature compressive plasticity in nanocrystal-toughened bulk copper-zirconium glass, *Philos. Mag. Lett.* 85 (2005) 221–229.
- [17] J. Das, M.B. Tang, K.B. Kim, R. Theissmann, F. Baier, W.H. Wang, J. Eckert, “Work-hardenable” ductile bulk metallic glass, *Phys. Rev. Lett.* 94 (2005), 205501.
- [18] D.H. Bae, M.H. Lee, D.H. Kim, Plasticity in $\text{Ni}_{59}\text{Zr}_{20}\text{Ti}_{16}\text{Si}_2\text{Sn}_3$ metallic glass matrix composites containing brass fibers synthesized by warm extrusion of powders, *Appl. Phys. Lett.* 83 (2003) 2312–2314.
- [19] H. Choi-Yim, R.D. Conner, W.L. Johnson, *In situ* composite formation in the Ni-(Cu)-Ti-Zr-Si system, *Scripta Mater.* 53 (2005) 1467–1470.
- [20] G. He, J. Eckert, W. Löser, Stability, phase transformation and deformation behavior of Ti-base metallic glass and composites, *Acta Mater.* 51 (2003) 1621–1631.
- [21] F.Q. Guo, H.J. Wang, S.J. Poon, G.J. Shiflet, Ductile titanium-based glassy alloy ingots, *Appl. Phys. Lett.* 86 (2005), 091907.
- [22] H. Ma, J. Xu, E. Ma, Mg-based bulk metallic glass composites with plasticity and high strength, *Appl. Phys. Lett.* 83 (2003) 2793–2795.
- [23] T. Wada, A. Inoue, A.L. Greer, Enhancement of room-temperature plasticity in a bulk metallic glass by finely dispersed porosity, *Appl. Phys. Lett.* 86 (2005), 251907.
- [24] B.L. Shen, H. Men, A. Inoue, Fe-based bulk glassy alloy composite containing *in situ* formed α -(Fe, Co) and $(\text{Fe, Co})_{23}\text{B}_6$ and microcrystalline grains, *Appl. Phys. Lett.* 89 (2006), 101915.
- [25] X. Li, H. Kato, K. Yubuta, A. Makino, A. Inoue, Effect of Cu on nanocrystallization and plastic properties of FeSiBPCu bulk metallic glasses, *Mater. Sci. Eng. A* 527 (2010) 2598–2602.
- [26] A. Takeuchi, A. Inoue, Classification of bulk metallic glasses by atomic size difference, heat of mixing and period of constituent elements and its application to characterization of the main alloying element, *Mater. Trans.* 46 (2005) 2817–2829.
- [27] O. Kubaschewski, J.F. Smith, D.M. Bailey, A thermodynamic analysis of phase relationships in the iron-copper system, *Z. Metallkd.* 68 (1977) 495–499.
- [28] M. Stoica, P. Ramasamy, I. Kaban, S. Scudino, M. Nicoara, G.B.M. Vaughan, J. Wright, R. Kumar, J. Eckert, Structure evolution of soft magnetic $(\text{Fe}_{36}\text{Co}_{36}\text{B}_{19.2}\text{Si}_{4.8}\text{Nb}_4)_{100-x}\text{Cu}_x$ ($x = 0$ and 0.5) bulk glassy alloys, *Acta Mater.* 95 (2015) 335–342.
- [29] P. Ramasamy, M. Stoica, A.H. Taghvaei, K.G. Prashanth, R. Kumar, J. Eckert, Kinetic analysis of the non-isothermal crystallization process, magnetic and mechanical properties of FeCoBSiNb and FeCoBSiNbCu bulk metallic glasses, *J. Appl. Phys.* 119 (2016), 073908.
- [30] M.W. Chen, A. Inoue, W. Zhang, T. Sakurai, Extraordinary plasticity of ductile bulk metallic glasses, *Phys. Rev. Lett.* 96 (2006), 245502.
- [31] F.E. Luborsky, *Amorphous Metallic Alloys*, Butterworth and Co (Publishers), London, UK, 1983.
- [32] T. Hamada, F.E. Fujita, Interference and pair correlation functions of crystalline embryo model of amorphous metals. II, *Jpn. J. Appl. Phys.* 24 (1985) 249–260.
- [33] X. Hui, D.Y. Lin, X.H. Chen, W.Y. Wang, Y. Wang, S.L. Shang, Z.K. Liu, Structural mechanism for ultrahigh-strength Co-based metallic glasses, *Scripta Mater.* 68 (2013) 257–260.
- [34] R. Li, M. Stoica, J. Eckert, Effect of minor Cu addition on phase evolution and magnetic properties of $\{[(\text{Fe}_{0.5}\text{Co}_{0.5})_{0.75}\text{Si}_{0.05}\text{B}_{0.20}]_{0.96}\text{Nb}_{0.04}\}_{100-x}\text{Cu}_x$ alloys, *J. Phys. Conf. Ser.* 144 (2009), 012042.